



Universiteit  
Leiden  
The Netherlands

## **The metallophilic interaction between cyclometalated complexes: photobiological applications**

Zhou, X.

### **Citation**

Zhou, X. (2021, May 26). *The metallophilic interaction between cyclometalated complexes: photobiological applications*. Retrieved from <https://hdl.handle.net/1887/3158746>

Version: Publisher's Version

License: [Licence agreement concerning inclusion of doctoral thesis in the Institutional Repository of the University of Leiden](#)

Downloaded from: <https://hdl.handle.net/1887/3158746>

**Note:** To cite this publication please use the final published version (if applicable).

Cover Page



Universiteit Leiden



The handle #<https://hdl.handle.net/1887/3158746> holds various files of this Leiden University dissertation.

**Author:** Zhou, X.

**Title:** The metallophilic interaction between cyclometalated complexes: photobiological applications

**Issue Date:** 2021-04-08

# 1

## **Introduction**

## 1.1 Anticancer metallodrugs

Metal-based materials have been on the basis of technology in the history of mankind. In recent decades, they have also shown important applications as therapeutics or for diagnostics, notably for cancer.<sup>1, 2</sup> Cancer is a general term encompassing many different diseases that all involve uncontrolled cell growth; it is one of the main health problems all over the world.<sup>3</sup> In 2017, the death of 9.6 million people was due to various forms of cancer.<sup>4</sup> This situation stimulates researchers to develop diverse methods for the treatment of cancer. In many aspects, metallodrugs have played a unique role in these developments. Cisplatin is a widely used chemotherapy medication against various types of cancer in clinical use since 1978.<sup>5</sup> Its success but also its limitations prompted the development of several alternative platinum-based anticancer drugs, including carboplatin, oxaliplatin, nedaplatin and heptaplatin (Figure 1.1a).<sup>6</sup> Cisplatin induces cancer cell death via binding to the purine bases of DNA (N7 of guanine and adenine), forming stable cross-links that bend duplex DNA and block its replication and transcription (Figure 1.1b).<sup>5, 7</sup>

Many metal ions and complexes have a natural aptitude for interacting with anionic DNA, because of their cationic characteristics, the properties of their coordination spheres, and their tunable redox, ligand-releasing, and photophysical properties.<sup>8, 9</sup> The first X-ray structure proving the binding of cisplatin to DNA was reported by the group of Lippard in 1995.<sup>10</sup> Cisplatin shows a specific mechanism, *i.e.* it binds to DNA through one or two coordination bonds. Besides coordination, metal-based anticancer drugs also may have other modes of interaction with DNA, for example, intercalation. Intercalators usually have a planar structure that can insert between the DNA base pairs, thus stabilizing the metallodrug-DNA complex via  $\pi$ - $\pi$  stacking. Square-planar metal complexes for example can intercalate between DNA base pairs, while octahedral complexes often achieve partial intercalation via planar aromatic heterocyclic ligands, or interact with several DNA bases by groove binding. For example, metal complexes derived from the ligand dppz (dipyrido[2,3-a:3',2'-c]phenazine) and its derivatives, are considered as standard DNA intercalators.<sup>11</sup> Barton's group established impressive work based on this ligand. In particular, they developed a series of metal-containing intercalators that specifically interact with mismatched DNA in cancer cells.<sup>12-14</sup> The Salder and Dyson groups also developed many organometallic anticancer complexes, especially based on the piano-stool scaffold, as DNA intercalators.<sup>15-17</sup>

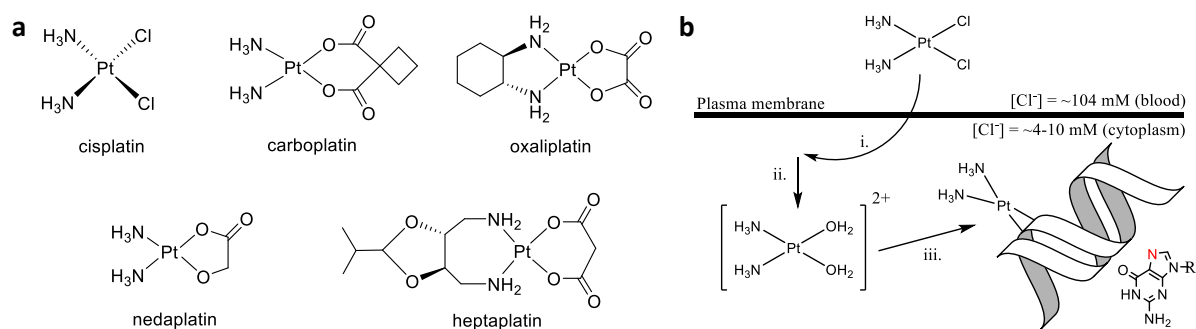


**Figure 1.1** (a) Platinum(II) complexes clinically used as cancer chemotherapy agents. (b) Classical view on the uptake (i), hydrolysis (ii) and DNA-binding of cisplatin.

DNA-targeting metallodrugs show significant anticancer ability. However, the poor selectivity of metal complexes for coordination to or intercalating into DNA, results in various off-target effects.<sup>18, 19</sup> Proteins, the main executors of the cell activity, often are alternative targets, which generates side effects. The combination of various metal ions with different coordination spheres, and the diversity and richness of available organic protein inhibitors, have generated a new era in the field of anticancer metallodrugs.<sup>6, 20</sup> Platinum and gold complexes have been studied first due to their optimal rate of ligand substitution reaction in biological environments; it even appeared possible to use them as multi-targeted anticancer agents.<sup>21, 22</sup> For example ethacraplatin, a Pt(IV) prodrug bound to two molecules of ethacrynic acid, a glutathione-S-transferase inhibitor, releases one molecule of cisplatin and two equivalents of ethacrynic acid after cellular uptake and intracellular reduction, which kills cancer cells via two different modes of action.<sup>23</sup> Gold(III) compounds can also be used that are usually reduced to gold(I) upon cellular uptake. These species show strong binding affinity to the thiol groups of many key biomolecules and enzymes inside a cell, such as glutathione (GSH), thioredoxin reductase (TrxR) or trypanothione reductase (TR), which are overexpressed in cancer cells because they control the redox balance of cells (Figure 1.2a).<sup>24-26</sup> Thus, many gold anticancer compounds disturb the redox level of cancer cells. In particular gold–NHC (N-heterocyclic carbene) complexes have attracted great attention for their stability under physiological conditions and their specific reactivity with TrxR proteins.<sup>22, 27</sup> Besides, Casini *et al.* also reported several gold(III) complexes showing selective inhibition of human aquaporins, which are positively correlated with tumor proliferation, migration, and angiogenesis.<sup>28, 29</sup> Altogether, these reports provide strong indications that gold complexes have high potential as anticancer (pro)drugs.

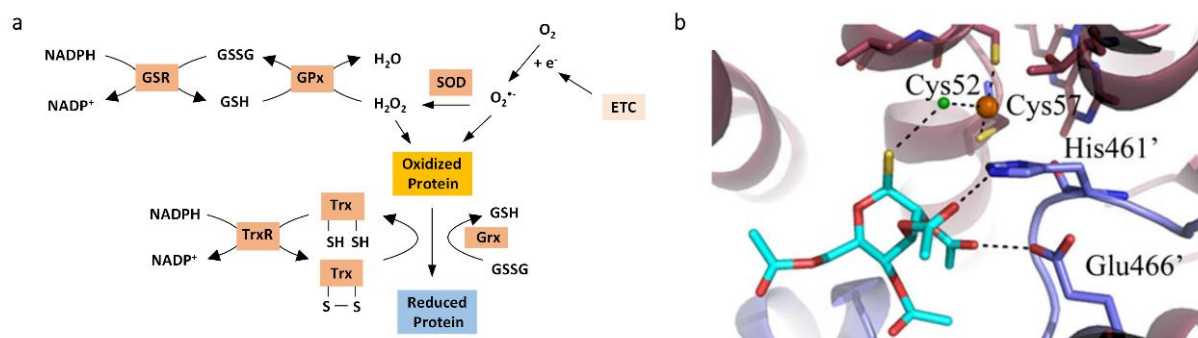


**Figure 1.2** (a) Scheme of the thioredoxin (TRx) system including substrate.<sup>24</sup> (b) CysS-Au(I)-SCys bond in TR-gold(I) adduct crystals (gold source auranofin).<sup>26</sup> The gold, chloride and sulfur ions are indicated in orange, green and yellow, respectively. The Cys52, Cys57, His461', Glu466' residues and the thiosugar moiety are represented as sticks.

## 1.2 Light in cancer treatment

The cytotoxicity and mode-of-action of DNA- or protein-targeting metal complexes have been thoroughly studied in the last few decades. However, many of the compounds tested in animals or humans still show toxicity to healthy tissues, because the biological molecules they target are also present in healthy cells, even if at a lower level than in cancer cells. Photodynamic therapy (PDT) is an alternative, non-invasive treatment developed to overcome the harmfulness of chemotherapy, radiation therapy, immunotherapy, or surgery, to healthy tissues.<sup>30</sup> In PDT, a photosensitizer (PS) is injected into human body. The PSs are designed to be non-toxic in the dark, but they can be activated upon accurate light irradiation at the tumor site. Upon absorption of light inside the cancer cells, the PS generates cytotoxic reactive oxygen species (ROS) that destroy the tumor structures and blood vessels via either a so-called Type I mechanism, which is more or less independent from the partial pressure of O<sub>2</sub> (pO<sub>2</sub>) in the irradiated tissues, or via a Type II mechanism, which is highly dependent on pO<sub>2</sub> (Figure 1.3).<sup>31-33</sup> The first step of type I and type II mechanisms are the same, *i.e.* the PS is excited to a singlet excited state <sup>1</sup>PS\* upon photon absorption, which interconverts to a triplet excited state <sup>3</sup>PS\* via intersystem crossing (ISC). In type I PDT, electron transfer happens between the triplet state <sup>3</sup>PS\* and substrate biomolecules, with the generation of free radicals and ROS in the sequential reaction chains.<sup>34</sup> In type II PDT, energy transfer occurs via triplet-triplet annihilation (TTA) between the triplet state <sup>3</sup>PS\* and the triplet ground state of dioxygen, <sup>3</sup>O<sub>2</sub>, to specifically produce singlet oxygen (<sup>1</sup>O<sub>2</sub>, excited state).<sup>35</sup> <sup>1</sup>O<sub>2</sub> is a highly reactive molecule that oxidizes proteins, lipids, and nucleic acids, which also generates ROS and ultimately causes cell death. Whether the PDT mechanism is type I or II, in PDT the precise irradiation at the tumor site generates an anticancer effect due

to massive ROS generation, while avoiding activation of the PS in the healthy tissues, and in parallel stimulating a systemic anti-cancer immune response.<sup>36, 37</sup>

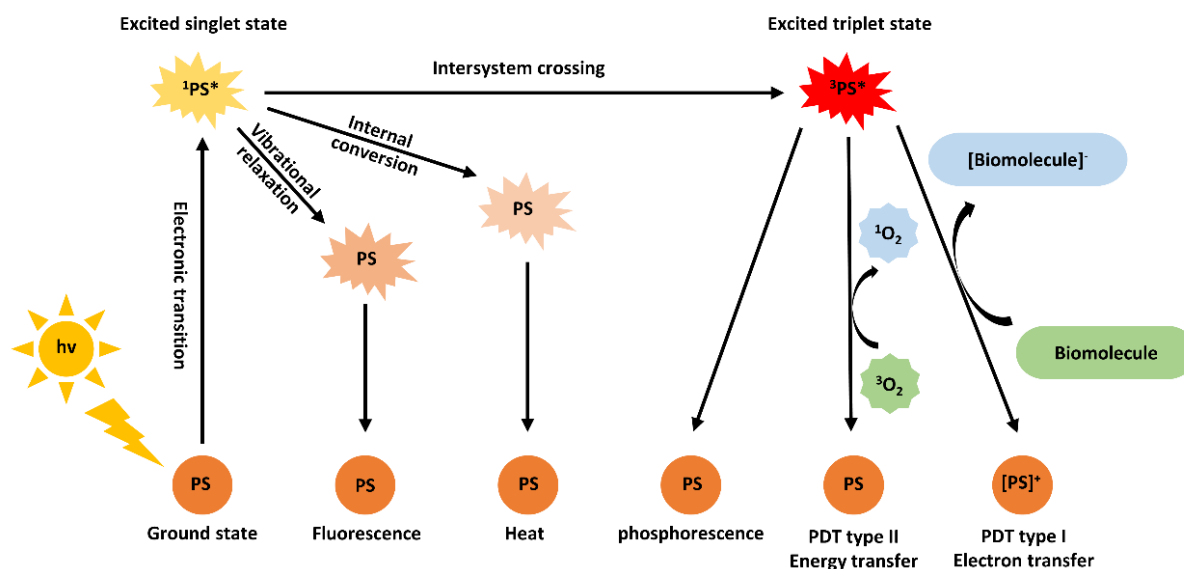


**Figure 1.3** Energy scheme and PDT mechanism of the photosensitizer (PS).

PDT treatment of cancer dates back to Ancient Egypt, India, and China, and it was reintroduced into modern society when the first PDT drug, Photofrin<sup>®</sup> (porfimer sodium) was approved by the U.S. Food and Drug Administration (FDA) in the 1990s.<sup>38</sup> In the last three decades, PDT has had a rapid development, with several new PSs being approved on the market. Photofrin<sup>®</sup> and HpD (Hematoporphyrin derivative), which belongs to the family of organic porphyrin compounds, are known as the first generation photosensitizers, characterized by high  $^1O_2$  quantum yields ( $\Phi_\Delta$ ).<sup>39</sup> The second-generation PSs have settled with lowering of the dark cytotoxicity, poorer light absorption in the visible region of the spectrum, and stronger light absorption in the far red or near infra-red region of the spectrum; they are still composed of organic molecules, such as chlorins, pheophorbides, *etc.*<sup>40</sup> Noticeably, introducing metal ions in the formula of the PS has emerged as a new design principle for the development of new and more efficient PDT agents.<sup>41</sup> Introduction of a heavy atom in a photosensitizer molecule generally facilitates intersystem crossing and improves the  $^1O_2$  quantum yield.<sup>42</sup> Palladium-based bacteriopheophorbide photosensitizer, WST09 (TOOKAD<sup>®</sup>) and WST11 (TOOKAD<sup>®</sup> soluble, Figure 1.4a), have been approved for prostate cancer treatment, and are in clinical trial for other forms of cancer; they show deeper tissue penetration and minimum skin photosensitivity compared with their organic analogues.<sup>43</sup> McFarland's group reported the ruthenium complex TLD1433 (Figure 1.4a), as the first Ru-based PDT agent that successfully completed phase Ib clinical trial.<sup>41, 44</sup> A recent report also demonstrated that several ruthenium

complexes could be active *in vivo* as two-photon PDT agents.<sup>45</sup> Those efforts make metal-based PSs a new generation of PDT agents.

The controlled ligand photosubstitution of  $d^6$  metal complexes has brought a new type of light-induced anticancer phototherapy, called photoactivated chemotherapy (PACT, Figure 1.4b).<sup>46-48</sup> In PACT, the biological effects of a cytotoxic moiety are inhibited in the dark by “caging” with a photocleavable protecting group. Upon irradiation with light, the photo-cleavable protecting group is released, for example via photosubstitution, which recovers the cytotoxicity of the anticancer moiety. PACT agents can be designed in three different ways: a non-toxic ligand is bound to a bioactive metal complex, the cancer-targeted cytotoxic ligand is bound to a non-active metal complex, or both the ligand and the metal complex are toxic after photosubstitution, which generates a dual mode of action.<sup>49, 50</sup> Our group recently synthesized a ruthenium-based PACT agent  $[\text{Ru}(\text{tpy})(\text{bpy})(\text{STF-31})]\text{Cl}_2$  based on STF-31, an organic enzyme inhibitor; this compound showed significantly increased cytotoxicity upon red-light triggered substitution of the STF31 inhibitor.<sup>51</sup> On the other hand, there are many PACT examples in which the toxic properties are attributed to the photogenerated metal complexes. Glazer and co-workers reported many ruthenium complexes, such as  $[\text{Ru}(\text{bpy})_2(\text{dmbpy})]\text{Cl}_2$  (Figure 1.4b), that after irradiation, release dmbpy to generate the supposedly cytotoxic species  $\text{cis-}[\text{Ru}(\text{bpy})_2(\text{OH}_2)_2]^{2+}$ ; the activated ruthenium complex then binds with DNA, which when occurring in cells, leads to a significant change of the half-maximal effective concentration ( $\text{EC}_{50}$ ) of the compound, from 136  $\mu\text{M}$  in the dark to 1.1  $\mu\text{M}$  after light irradiation in A549 cancer cells.<sup>52</sup>



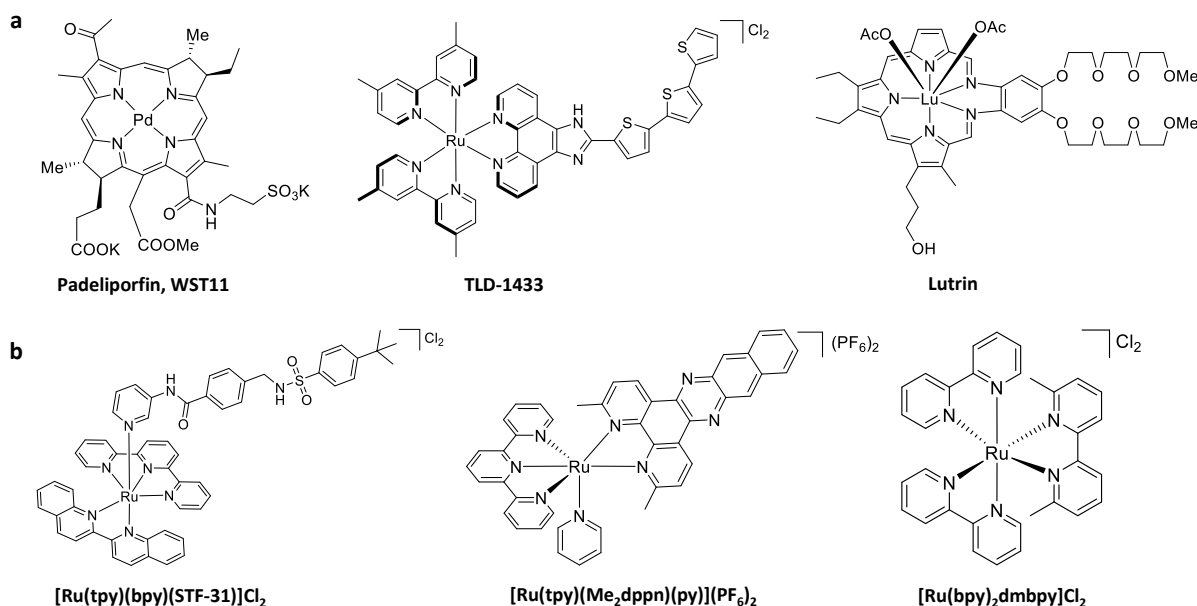


**Figure 1.4** (a) Three inorganic photosensitizers for PDT currently in clinical trial: padeliporfin (WST-11), TLD-1433, and lutetium texaphyrin (lutrin).<sup>46</sup> (b) Three reported PACT ruthenium complexes.

### 1.3 Cyclometalated complex in cancer treatment

Cyclometalation is defined as the transition metal center activates a C-R bond of organic ligand to form a metallacycle including a new metal-carbon  $\sigma$  bond.<sup>53</sup> This family of metal complexes emerges as extremely promising for catalytic, biochemical, and photochemical applications.<sup>54</sup> Cyclometalated complexes of the platinum group metals comprising Ru, Os, Rh, Ir, Pd, and Pt, have received the most attention.<sup>56</sup> The M-C bond involves a negatively charged carbon center that has strong  $\sigma$ -donating character, which makes it often stronger than classical M-X coordination bonds involving  $\pi$ -donating or  $\pi$ -accepting ligands based on heteroatoms (X = nitrogen, oxygen, sulfur, phosphorus, or halogen). This stronger coordination of cyclometalated ligands usually results in more stable complexes in (aqueous) physiological conditions, which is particularly relevant for metal-based drugs. Cyclometalation also lowers the overall charge of a metal complex, resulting in increased lipophilicity and thus usually in higher cellular uptake.<sup>57</sup> Based on these advantages, cyclometalated complexes have attracted considerable attention for anticancer treatment.<sup>58</sup> Chao *et al.* reported a thorough comparison between polypyridyl ruthenium(II) complexes and their cyclometalated analogs, by testing their anticancer activities against 2D and 3D cancer models.<sup>57</sup> This study demonstrated that compared with their polypyridyl analogs, cyclometalated ruthenium(II) complexes exhibit higher lipophilicity and better cellular uptake, with a much lower  $EC_{50}$  in 2D and 3D cancer models.

In PDT before a photon can excite the photosensitizer *in vivo*, it has to penetrate human tissues. It is well-known that light with a longer wavelength has better tissue penetration.<sup>43</sup> The presence of an M-C bond in principle lowers the HOMO-LUMO gap of metal complexes, leading to a bathochromic shift of their absorption spectrum to reach the photodynamic window (600-900 nm),<sup>59</sup> which is the key for PDT and PACT applications.<sup>60-62</sup> Cyclometalated iridium and Platinum complexes derived from polypyridyl ligands are particularly attractive for their low-energy metal-to-ligand charge-transfer (MLCT) excited states, which makes them good absorbers of visible light (Figure 1.5).<sup>62</sup> Peter and coworkers reported a cyclometalated iridium complex that showed photoredox catalysis in cancer cells upon blue light irradiation with an oxygen-independent mechanism of action.<sup>63</sup> The group of Mao reported a series of cyclometalated iridium complexes that acted as lysosome-targeted photodynamic anticancer and real-time tracking agents, presenting cyclometalated complexes as a new kind of theranostic compounds.<sup>64</sup> Huang *et al.* introduced a coumarin group into a cyclometalated ruthenium complex, thereby affording an efficient type I PDT agent active under white light activation.<sup>65</sup> Our group synthesized a heteroleptic cyclometalated ruthenium complex that underwent selective photosubstitution of a bidentate ligand, indicating that a cyclometalated complex may be developed with interesting PACT properties.<sup>66</sup> There are also many cyclometalated platinum-, palladium- and gold-based photosensitizers for PDT.<sup>42, 67, 68</sup> Sarli *et al.* combined the cyclic peptide c(RGDyK) with a cyclometalated platinum scaffold to successfully achieve PDT treatment of rat bladder cancer cells.<sup>69</sup> The Zou groups recently reported that cyclometalated gold(III)-hydride complexes act as potent photoactivated anticancer agents based on their visible-light-induced thiol reactivity.<sup>70</sup> In conclusion, the advantageous properties of cyclometalated complexes bring a new era of bioinorganic chemistry with respect to anticancer treatment.

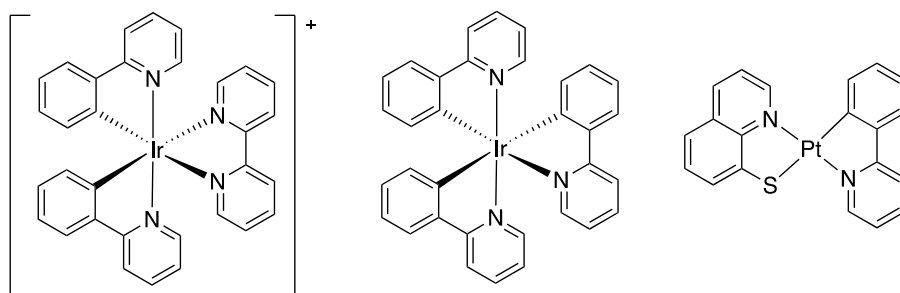


**Figure 1.5** The structures of three cyclometalated photosensitizers used in PDT.<sup>67</sup>

## 1.4 Metallophilic interactions

Several transition metals (M) can be engaged in metallophilic M...M interaction resulting in subsequent self-assembly behavior,<sup>55</sup> which has brought several fascinating studies in supramolecular bioinorganic chemistry. The metallophilic interaction typically occurs for  $d^8$  and  $d^{10}$  square-planar or linear transition metal complexes. It drives molecules to self-assemble into aggregates that minimize the metal...metal distances below 3.5-4.0 Å. This self-assembly dramatically modifies the properties of the metal compound compared to the non-aggregated monomer, for example by enhancing its luminescence, increasing its excited-state lifetime, or reducing its chemical reactivity.<sup>71</sup> This phenomenon has allowed for the creation of a new category of light-emitting self-assembled materials.<sup>55</sup> Meanwhile, the versatility in ligand structures and metal coordination spheres has facilitated the making of a large range of self-assembled nanostructures and molecular topologies based on metal complexes showing metallophilic interactions (Figure 1.6).<sup>72</sup> To assess the existence of this interaction, the most direct method is X-ray crystal structure determination, which shows the distance between metal centers. If the metal...metal distance is shorter than the sum of van der Waals radius of the metal cations, it is reasonable to assume the existence of metal...metal interaction. Another common method is to compare the spectroscopic properties of the metal complex in its self-assembled polymeric and monomeric states, which usually resemble the spectra of their solid and solution states, respectively.<sup>73</sup>

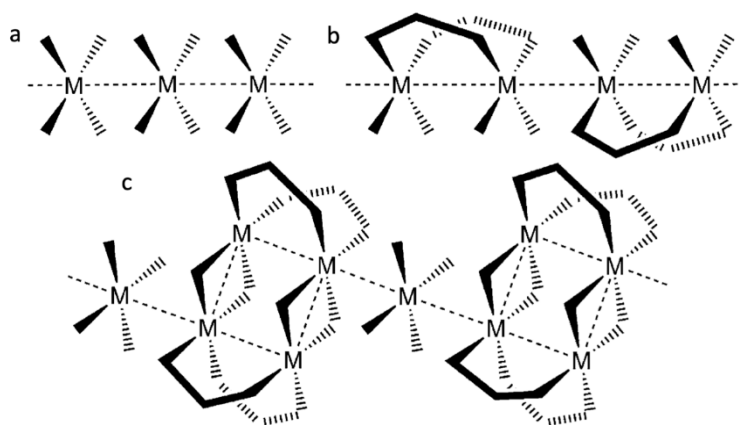


**Figure 1.6** Schematic drawing of metal complexes showing a metallophilic interaction. (a) linear chain composed of square planar molecules. (b) linear chain composed of paddlewheel molecules. (c) mixture motifs.<sup>72</sup>

The most simple self-assembly *via* metallophilic interaction is obtained when the metal complexes form a linear infinite chain of molecules directly interacting with two neighboring

metal centers.<sup>74</sup> Typical examples of such systems are formed by  $d^8$  transition metal complexes, especially Pt(II) complexes.<sup>71, 75</sup> The square-planar coordination geometry provided by Pt(II) and the attractive spectroscopic and photophysical properties of complexes based on this metal have been well documented; besides, these complexes are particularly prone to generating intermolecular Pt...Pt interaction.<sup>76</sup> Specifically, the Pt...Pt interaction is attributed to the closed-shell electronic overlap between the axial  $d_z^2$  orbitals, often combined with  $\pi$ - $\pi$  stacking of the flat aromatic ligands coordinated to platinum. The orbital interaction between the  $d_z^2$  orbitals induces a new  $d_z^2$  hybridization in the polymeric form, leading to a change of the highest occupied molecular orbital (HOMO). While the stabilized bonding combination of the  $d_z^2$  orbital on both metal centers usually ends up in lower, 2-electron filled molecular orbitals, their destabilized anti-bonding combination, often mixed with  $\pi$  orbital of the ligand(s), gives rise to a new HOMO molecular orbital, while the LUMO is formed by combinations of  $\pi^*$  orbitals of the ligand(s). The resulting low-energy optical transition, from the metal  $d\sigma^*$  HOMO to the ligand  $\pi^*$  orbitals LUMO, leads to metal-metal-to-ligand charge transfer (MMLCT) excited states and a lower HOMO-LUMO gap, compared to the either ligand-centered (LC) or metal-to-ligand charge transfer (MLCT) transitions usually observed with the parent monomer molecules (Figure 1.7a).<sup>75</sup> For platinum complexes, this new transition translates into low-energy absorbance and emission bands, typically in the red or even near-infrared region of the spectrum. A common self-assembly system is the cyclometalated cationic pincer-type Pt(II) complexes (Figure 1.7b).<sup>77</sup> Cyclometalation lowers the electrostatic repulsion between the Pt(II) centers, while the planar structure of the ligand prevents steric hindrance to occur, which allows  $\pi$ - $\pi$  stacking to occur and altogether results in short Pt...Pt distances and rather strong Pt-Pt interactions. The occurrence of self-assembly with such complexes is typically accompanied by the generation of nanorods or nanofibers in mixed solvent systems, and deep-red emission in the aggregated form.<sup>78, 79</sup> The de Cola group established a system where the self-assembly of luminescent Pt(II) complexes could be controlled, which allowed the authors to achieve diagnostic and biosensing functions in such systems.<sup>80</sup>

Palladium is in the same group as platinum in the periodic table of the elements, and Pd(II) thus has similar  $d^8$  square-planar structures. Indeed, several cyclometalated cationic pincer-type Pd(II) complexes were shown to exhibit metallophilic interactions and to form similar self-assembled nanostructures as that obtained with Pt analogs (Figure 1.7b).<sup>81, 82</sup> However, also being a lighter metal center, Pd(II) usually makes complexes with a fainter phosphorescence because of the less efficient inter-system crossing (ISC) and slower  $T_1$ - $S_0$  radiative decay.<sup>83</sup> As

a result, limited attention has been paid to Pd(II)-based light-emitting materials.<sup>84</sup> Au(III) complexes, which are isoelectronic to those of Pt(II) or Pd(II), have recently been reported to show self-assembly via aurophilic interaction, thereby introducing a new molecular building block capable of developing metallophilic interactions (Figure 1.7c).<sup>85</sup> However, the applications based on these new self-assembled nanostructures are still in a primary exploration stage.

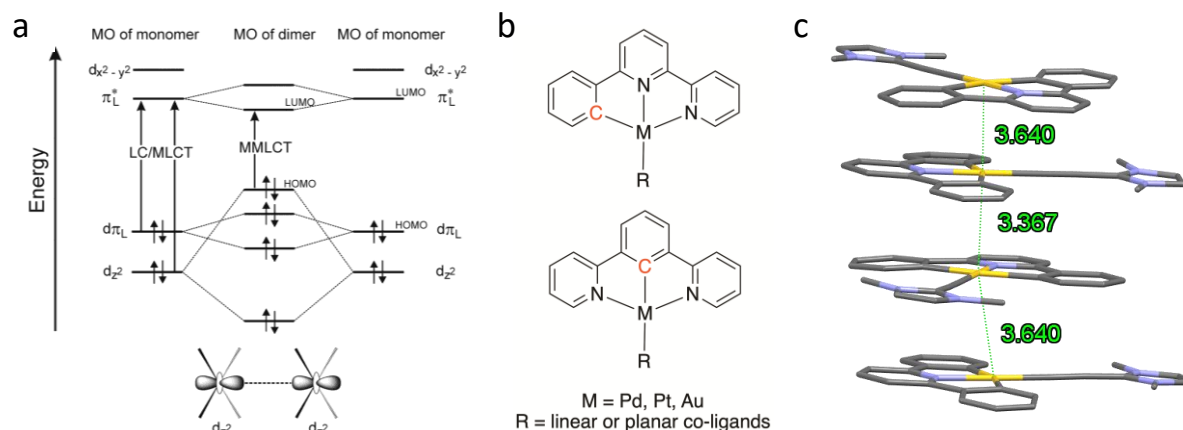


**Figure 1.7** (a) Simplified MO diagram of two interacting square-planar platinum(II) complexes, showing the overlap of the  $d_{z^2}$  orbital of each metal fragment, and its influence on the energy of the molecular orbital levels of the dimer.<sup>71</sup> (b) Typical molecular structures of self-assembling systems based on the metallophilic interaction. (c) A unidirectional supramolecular chain as an example of an Au(III) complex involved in aurophilic interaction (distance unit Å).<sup>85</sup>

## 1.5 Metals in nanomedicine

In 2002, the US National Institutes of Health (NIH) started a new research program to apply nanoscience and nanotechnology in medicine, leading to the emergence of a new field called nanomedicine.<sup>86</sup> Nanomedicine aims to achieve diagnosis and treatment of diseases via the specific properties of nanomaterials.<sup>87</sup> Cancer therapy is one of the main research areas of the previously unimaginable development of modern nanomedicine. Researchers found that many nanoparticles (NPs) exhibit the so-called “enhanced permeation and retention” (EPR) effect, which makes them more efficiently taken up in tumor tissues than in normal tissues.<sup>88, 89</sup> The blood vessel at the tumor microenvironment is leakier than that of healthy tissues,<sup>90</sup> making nanoparticles cross the tumor blood vessels in a high opportunity compared with the healthy tissues. Moreover, The nanostructures may also protect the drug from recognition and clearance before reaching the target,<sup>91</sup> thus providing long circulation times that may be accompanied by

an efficient delivery to the target. The EPR effect has stimulated the application of NPs as drug delivery systems to solid tumors,<sup>92</sup> However, EPR effect has also been recently discussed extensively in the literature for application in human medicine.<sup>93-95</sup> A recent research convinces that the active process through endothelial cells, instead of the tumor blood vessels gaps, is majorly responsible for the entry of nanoparticles into solid tumors, which challenges the conventional rationale of EPR effect for developing cancer nanomedicine.<sup>93</sup>

Nanoparticles have been used in studies concerning bioimaging, drug delivery and phototherapy.<sup>96</sup> Many simple molecules, although they may have excellent photophysical properties for PDT as monomers, are often too hydrophobic to be used in medicine without chemical modification, as they typically aggregate in serum or tumor cells into PDT-inactive aggregates. The conjugation of PDT molecules to NPs has been proposed for solving these problems. The NP coating strategy can easily generate PDT drugs uniformly distributed in aqueous solutions. Based on this research, Hsiao *et al.* developed a  $\text{Fe}_3\text{O}_4/\text{SiO}_2$  core/shell nanocomposite that conjugated a functionalized iridium photosensitizer for cell imaging and anticancer PDT treatment.<sup>97</sup> Recently, the Chen group reviewed the development of ruthenium complexes from single-molecule compounds to nanoparticles.<sup>98</sup> The Gasser group has developed several polymers encapsulated metal complexes with significant PDT effect, suggesting a promising future for the nanoconjunction of metal complexes..<sup>88, 99</sup>

Many nanoparticles include metal centers (Figure 1.8).<sup>100</sup> A well-known category of such NPs comprise gold nanoparticles (AuNPs), which are made by fully reduced  $\text{Au}^0$  atoms.<sup>101</sup> Generally, AuNPs are stabilized using thiolate moieties that form strong Au–S bond between the soft Lewis acid Au and the soft thiolate Lewis base (S). One of the specificities of AuNPs is that they have a significant surface plasmon resonance (SPR) mode in the visible region of the spectrum if one of their dimensions is much smaller than the wavelength of the light used to excite them.<sup>102</sup> Light irradiation at the SPR wavelength of AuNPs is usually followed by fast conversion of the photon energy into heat.<sup>102</sup> The SPR absorption of many AuNPs is matching ideally with the first phototherapy window (650-900 nm), making AuNPs highly promising photothermal therapy (PTT) materials in cancer treatment.<sup>103</sup> On the imaging side, many nanoparticles bound specifically to gadolinium complexes have been investigated as contrast agents (CAs) in magnetic resonance imaging (MRI).<sup>104</sup> Ample works have also focussed on the use of  $\text{Ln}^{3+}$ -doped upconversion nanoparticles (Ln-UCNPs) both for diagnostic sensing (bioimaging), disease treatment (therapy), or both (theranostic). The upconversion properties of these Ln-UCNPs is based on the specific properties of 4f electronic levels in lanthanoid metal

centers; many dedicated reviews have been written on this well-developed chemistry.<sup>105-107</sup> Ln-UCNPs have received particular attention in the field of optical imaging for their high resistance to photobleaching and near-infrared (NIR) excitation, which results in deeper penetration of the exciting light into biological tissues, compared to traditional organic dyes that require visible or UV excitation.<sup>108</sup> Our group has developed a UCNP nanosystem combining lanthanoid upconversion with photocleavable ruthenium complexes, to achieve NIR activation of the ruthenium prodrugs.<sup>109</sup> Overall, these efforts suggest that metal atoms and complexes play an important contribution to the development of nanomedicine.

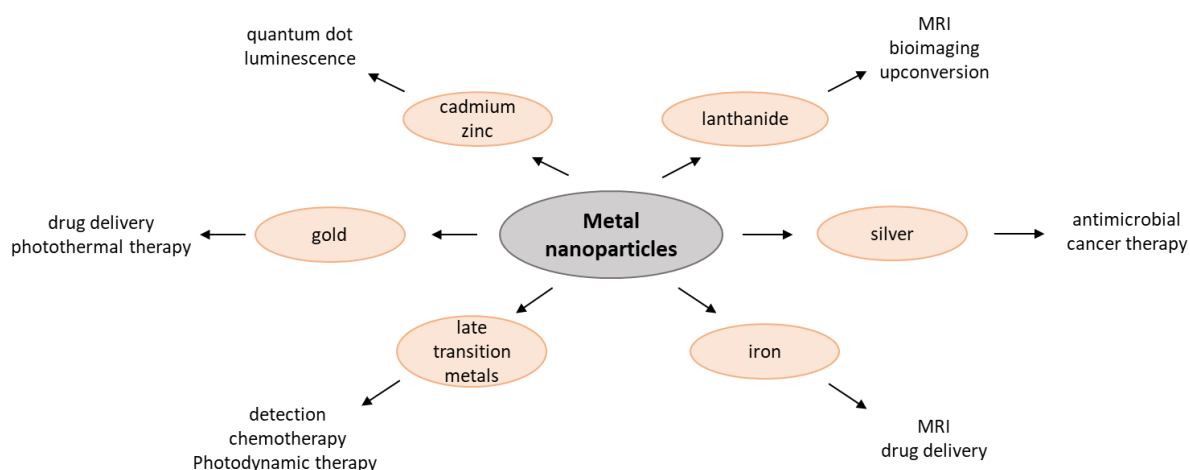


**Figure 1.8** Different types of metal nanoparticles and their biological application.

## 1.6 Aim and outline of this thesis

The studies described above give a short overview of the use of metals in cancer treatment, from metallodrugs to metal-based photosensitizers for PDT and metal-based nanomedicine platforms. However, so far limited research has been dedicated to the self-assembly of molecular photosensitizers into well-defined nanoparticles, and on the evaluation of these aggregates as anticancer compounds. The goal of the research described in this thesis is the exploration of the molecular and supramolecular chemistry of  $d^8$  metal-based PDT sensitizers, and specifically those based on the tetradentate cyclometalating ligands shown in Figure 1.9.

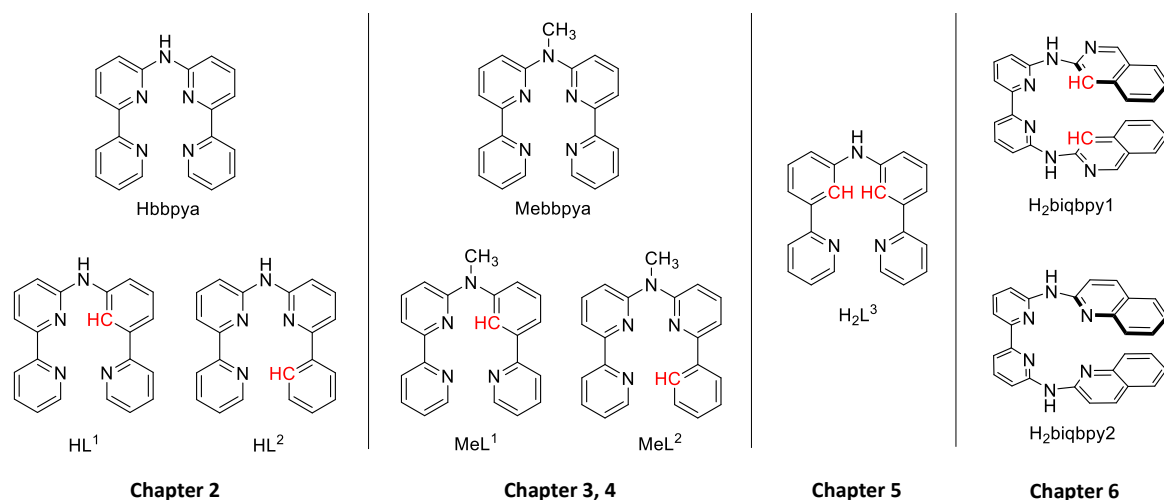


**Figure 1.9** The chemical structures of tetrapyridyl and cyclometalating tetradentate ligands described in this thesis.

In **chapter 2**, the chemistry and photochemistry of two isomeric cyclometalated palladium complexes based on the **HL**<sup>1</sup> and **HL**<sup>2</sup> ligands are described. In particular, blue-light PDT properties were discovered for only one of these isomers, and the role of the position of the Pd-C bond on the photochemical properties of these complexes is discussed in more details using a combination of experiments and theoretical calculations.

In **chapter 3**, the non-coordinated N bridge of the **HL**<sup>1</sup> and **HL**<sup>2</sup> ligands studied in **chapter 2**, was methylated and the resulting ligands **MeL**<sup>1</sup> and **MeL**<sup>2</sup> coordinated to palladium(II). By doing so, the NH deprotonation described in **chapter 2**, was made impossible, which allowed for exploring in more detail the self-assembly of these cyclometalated complexes, and to compare it to that of their tetrapyridyl analogue complex based on the Hbbpya ligand (Figure 1.9). The photophysical, photochemical, and photobiological properties of these three molecules were found to highly depend on their self-assembly in biological conditions, which depended dramatically on the presence of proteins in the aqueous medium. Their applications as PDT agents are compared in *in vitro* and *in vivo* cancer models.

In **chapter 4**, the **MeL**<sup>1</sup> and **MeL**<sup>2</sup> described in **chapter 3** were coordinated to platinum(II), and the photophysical, photochemical, supramolecular, and (photo)biological properties of the resulting two isomer complexes, were studied in detail. Contrary to the palladium complexes studied in **chapter 3**, which were good PDT agents but poor emitters, these platinum-based cyclometalated complexes were found to be weak PDT agents, but very interesting emitters. The self-assembly observed due to the Pt...Pt interaction indeed stimulated red absorption and deep-red emission, which allowed us to monitor in time and space the uptake and distribution



of the nanostructures generated by these complexes in cancer cells. This study brings new perspectives to a new type of theranostic nanoplatform that targets mitochondria.

In **chapter 5**, a biscyclometalated analogue palladium complex, related to the one described in **chapter 2** and using the ligand **H<sub>2</sub>L<sup>3</sup>**, is reported. This complex showed particularly efficient green-light-activated PDT properties not only under normoxia but also in hypoxic cancer cells, as characterized by high photoindex (PI) *in vitro* and excellent antitumor effects in a mice model of skin melanoma. The combination of the excellent PDT properties of this complex and its self-assembly into nanoparticles *via* the metallophilic interaction, results in a new tumor-targeting strategy for PDT that uses a molecular PS to generate nanoparticles *in vivo*, without a need for chemical conjugation to known tumor-targeting nanoplatforms. To name this new strategy we propose the term “molecular photosensitizer self-assembled nanoparticles”, or MoPSAN; in this chapter it was used to achieve hypoxia tumor inhibition.

In **chapter 6**, a gold(III) biscyclometalated complex was serendipitously obtained *via* the so-called “rollover” effect during the coordination of the tetrapyrrolyl ligand **H<sub>2</sub>biqbpy1**. Rollover cyclometalation is a specific coordination reversal of polypyridyl ligands, from the common M-N bond coordination to the meta M-C bond in the same heterocyclic ring, which becomes deprotonated. This effect is strongly dependent on the structure of the ligand, as an isomer of the ligand, **H<sub>2</sub>biqbpy2**, led to the expected tetrapyrrolyl gold(III) complex. The cytotoxicity of both complexes towards different types of cancer cells was investigated, and rationalized by looking at their reactivity towards thiol-containing compounds, their TrxR inhibition properties, and their potassium channel binding affinity.

Finally, in **chapter 7**, a summary is presented for the main findings described in this thesis, followed by a general discussion, and an outlook for further research.

## 1.7 References

1. K. H. Thompson and C. Orvig, *Science*, 2003, **300**, 936-939.
2. K. J. Franz and N. Metzler-Nolte, *Chem. Rev.*, 2019, **119**, 727-729.
3. R. L. Siegel, K. D. Miller and A. Jemal, *CA Cancer J. Clin.*, 2019, **69**, 7-34.
4. M. Naghavi, A. A. Abajobir, A. D. Lopez and C. J. L. Murray, *Lancet*, 2017, **390**, 1151-1210.
5. S. Dasari and P. Bernard Tchounwou, *Eur. J. Pharmacol.*, 2014, **740**, 364-378.
6. R. G. Kenny and C. J. Marmion, *Chem. Rev.*, 2019, **119**, 1058-1137.
7. C. R. Rocha, M. M. Silva, A. Quinet, J. B. Cabral-Neto and C. F. Menck, *Clinics*, 2018, **73**.
8. L. J. K. Boerner and J. M. Zaleski, *Curr. Opin. Chem. Biol.*, 2005, **9**, 135-144.
9. A. C. Komor and J. K. Barton, *Chem. Commun.*, 2013, **49**.
10. P. M. Takahara, A. C. Rosenzweig, C. A. Frederick and S. J. Lippard, *Nature*, 1995, **377**, 649-652.
11. A. W. McKinley, P. Lincoln and E. M. Tuite, *Coord. Chem. Rev.*, 2011, **255**, 2676-2692.

12. A. N. Boynton, L. Marcélis and J. K. Barton, *J. Am. Chem. Soc.*, 2016, **138**, 5020-5023.
13. K. M. Boyle and J. K. Barton, *J. Am. Chem. Soc.*, 2018, **140**, 5612-5624.
14. H. Song, J. T. Kaiser and J. K. Barton, *Nat. Chem.*, 2012, **4**, 615-620.
15. H. K. Liu and P. J. Sadler, *Acc. Chem. Res.*, 2011, **44**, 349-359.
16. Y. K. Yan, M. Melchart, A. Habtemariam and P. J. Sadler, *Chem. Commun.*, 2005, **38**, 4764-4776.
17. Z. Ma, G. Palermo, Z. Adhireksan, B. S. Murray, T. V. Erlach, U. R. Paul J. Dyson and C. A. Davey., *Angew. Chem. Int. Ed.*, 2016, **55**, 7441-7444.
18. A.-M. Florea and D. Büsselberg, *Cancers*, 2011, **3**, 1351-1371.
19. C. Santini, M. Pellei, V. Gandin, M. Porchia, F. Tisato and C. Marzano, *Chem. Rev.*, 2013, **114**, 815-862.
20. D.-L. Ma, D. S.-H. Chan and C.-H. Leung, *Acc. Chem. Res.*, 2014, **47**, 3614-3631.
21. T. C. Johnstone, K. Suntharalingam and S. J. Lippard, *Chem. Rev.*, 2016, **116**, 3436-3486.
22. M. Mora, M. C. Gimeno and R. Visbal, *Chem. Soc. Rev.*, 2019, **48**, 447-462.
23. W. H. Ang, I. Khalaila, C. S. Allardyce, L. Juillerat-Jeanneret and P. J. Dyson, *J. Am. Chem. Soc.*, 2005, **127**, 1382-1383.
24. K. Nakao, N. Minato and S. Uemoto, *Innovative medicine: basic research and development*, Springer Nature, 2015.
25. T. Zou, C. T. Lum, C.-N. Lok, J.-J. Zhang and C.-M. Che, *Chem. Soc. Rev.*, 2015, **44**, 8786-8801.
26. A. Ilari, P. Baiocco, L. Messori, A. Fiorillo, A. Boffi, M. Gramiccia, T. Di Muccio and G. Colotti, *Amino Acids*, 2012, **42**, 803-811.
27. J. L. Hickey, R. A. Ruhayel, P. J. Barnard, M. V. Baker and S. J. Berners-Price, *J. Am. Chem. Soc.*, 2008, **130**, 12570-12571.
28. A. de Almeida, A. F. Mosca, D. Wragg, M. Wenzel, P. Kavanagh, G. Barone, S. Leoni, G. Soveral and A. Casini, *Chem. Commun.*, 2017, **53**, 3830-3833.
29. B. Aikman, A. de Almeida, S. M. Meier-Menches and A. Casini, *Metallomics*, 2018, **10**, 696-712.
30. P. Agostinis, K. Berg, K. A. Cengel, T. H. Foster, A. W. Girotti, S. O. Gollnick, S. M. Hahn, M. R. Hamblin, A. Juzeniene, D. Kessel, M. Korbelik, J. Moan, P. Mroz, D. Nowis, J. Piette, B. C. Wilson and J. Golab, *CA Cancer J. Clin.*, 2011, **61**, 250-281.
31. F. Hu, S. Xu and B. Liu, *Adv. Mater.*, 2018, **30**.
32. J. Li and K. Pu, *Chem. Soc. Rev.*, 2019, **48**, 38-71.
33. A. Gorman, J. Killoran, C. O'Shea, T. Kenna, W. M. Gallagher and D. F. O'Shea, *J. Am. Chem. Soc.*, 2004, **126**, 10619-10631.
34. S. Kwiatkowski, B. Knap, D. Przystupski, J. Saczko, E. Kędzierska, K. Knap-Czop, J. Kotlińska, O. Michel, K. Kotowski and J. Kulbacka, *Biomed. Pharmacother.*, 2018, **106**, 1098-1107.
35. L. B. Josefsen and R. W. Boyle, *Met. Based Drugs*, 2008, **2008**, 1-23.
36. F. Anzengruber, P. Avci, L. F. de Freitas and M. R. Hamblin, *Photochem. Photobiol. Sci.*, 2015, **14**, 1492-1509.
37. I. Beltran Hernandez, Y. Yu, F. Ossendorp, M. Korbelik and S. Oliveira, *J. Clin. Med.*, 2020, **9**.
38. A. B. Ormond and H. S. Freeman, *Materials*, 2013, **6**, 817-840.
39. S. K. Pushpan, S. Venkatraman, V. G. Anand, J. Sankar, D. Parmeswaran, S. Ganesan and T. K. Chandrashekar, *Anti-Cancer Agents Med. Chem.*, 2002, **2**, 187-207.
40. H. Kataoka, H. Nishie, N. Hayashi, M. Tanaka, A. Nomoto, S. Yano and T. Joh, *Ann. Transl. Med.*, 2017, **5**, 183.
41. S. Monro, K. L. Colón, H. Yin, J. Roque, P. Konda, S. Gujar, R. P. Thummel, L. Lilge, C. G. Cameron and S. A. McFarland, *Chem. Rev.*, 2018, **119**, 797-828.
42. M. Obata, S. Hirohara, R. Tanaka, I. Kinoshita, K. Ohkubo, S. Fukuzumi, M. Tanihara and S. Yano, *J. Med. Chem.*, 2009, **52**, 2747-2753.
43. A. E. O'Connor, W. M. Gallagher and A. T. Byrne, *Photochem. Photobiol. Sci.*, 2009, **85**, 1053-1074.
44. P. Kaspler, S. Lazic, S. Forward, Y. Arenas, A. Mandel and L. Lilge, *Photochem. Photobiol. Sci.*, 2016, **15**, 481-495.

45. J. Karges, S. Kuang, F. Maschietto, O. Blacque, I. Ciofini, H. Chao and G. Gasser, *Nat. Commun.*, 2020, **11**, 3262.
46. S. Bonnet, *Dalt. Trans.*, 2018, **47**, 10330-10343.
47. V. H. S. van Rixel, B. Siewert, S. L. Hopkins, S. H. C. Askes, A. Busemann, M. A. Siegler and S. Bonnet, *Chem. Sci.*, 2016, **7**, 4922-4929.
48. V. H. S. van Rixel, V. Ramu, A. B. Auyeung, N. Beztsinna, D. Y. Leger, L. N. Lameijer, S. T. Hilt, S. E. Le Devedec, T. Yildiz, T. Betancourt, M. B. Gildner, T. W. Hudnall, V. Sol, B. Liagre, A. Kornienko and S. Bonnet, *J. Am. Chem. Soc.*, 2019, **141**, 18444-18454.
49. J. A. Cuello-Garibo, M. S. Meijer and S. Bonnet, *Chem. Commun.*, 2017, **53**, 6768-6771.
50. J. D. Knoll, B. A. Albani and C. Turro, *Chem. Commun.*, 2015, **51**, 8777-8780.
51. L. N. Lameijer, D. Ernst, S. L. Hopkins, M. S. Meijer, S. H. C. Askes, S. E. Le Dévedec and S. Bonnet, *Angew. Chem. Int. Ed.*, 2017, **56**, 11549-11553.
52. B. S. Howerton, D. K. Heidary and E. C. Glazer, *J. Am. Chem. Soc.*, 2012, **134**, 8324-8327.
53. M. Albrecht, *Chem. Rev.*, 2010, **110**, 576-623.
54. D. Ma, T. Tsuboi, Y. Qiu and L. Duan, *Adv. Mater.*, 2017, **29**.
55. V. W. Yam, V. K. Au and S. Y. Leung, *Chem. Rev.*, 2015, **115**, 7589-7728.
56. M. Albrecht, *Chem. Rev.*, 2010, **110**, 576-623.
57. H. Huang, P. Zhang, H. Chen, L. Ji and H. Chao, *Chem. Eur. J.*, 2015, **21**, 715-725.
58. P. Zhang and P. J. Sadler, *J. Organomet. Chem.*, 2017, **839**, 5-14.
59. S. Bonnet, *Comment Inorg. Chem.*, 2014, **35**, 179-213.
60. P. G. Bomben, K. C. Robson, P. A. Sedach and C. P. Berlinguette, *Inorg. Chem.*, 2009, **48**, 9631-9643.
61. X. Q. Zhou, A. Busemann, M. S. Meijer, M. A. Siegler and S. Bonnet, *Chem. Commun.*, 2019, **55**, 4695-4698.
62. S. L. Higgins and K. J. Brewer, *Angew. Chem. Int. Ed.*, 2012, **51**, 11420-11422.
63. H. Huang, S. Banerjee, K. Qiu, P. Zhang, O. Blacque, T. Malcomson, M. J. Paterson, G. J. Clarkson, M. Staniforth, V. G. Stavros, G. Gasser, H. Chao and P. J. Sadler, *Nat. Chem.*, 2019, **11**, 1041-1048.
64. L. He, Y. Li, C.-P. Tan, R.-R. Ye, M.-H. Chen, J.-J. Cao, L.-N. Ji and Z.-W. Mao, *Chem. Sci.*, 2015, **6**, 5409-5418.
65. Z. Lv, H. Wei, Q. Li, X. Su, S. Liu, K. Y. Zhang, W. Lv, Q. Zhao, X. Li and W. Huang, *Chem. Sci.*, 2018, **9**, 502-512.
66. J. A. Cuello-Garibo, C. C. James, M. A. Siegler, S. L. Hopkins and S. Bonnet, *Chem. Eur. J.*, 2019, **25**, 1260-1268.
67. X. Jiang, N. Zhu, D. Zhao and Y. Ma, *Sci. China Chem.*, 2015, **59**, 40-52.
68. N. M. Shavaleev, H. Adams, J. Best, R. Edge, S. Navaratnam and J. A. Weinstein, *Inorg. Chem.*, 2006, **45**, 9410-9415.
69. T. Chatzisideri, S. Thysiadis, S. Katsamakos, P. Dalezis, I. Sigala, T. Lazarides, E. Nikolakaki, D. Trafalis, O. A. Gederaas, M. Lindgren and V. Sarli, *Eur. J. Med. Chem.*, 2017, **141**, 221-231.
70. H. Luo, B. Cao, A. S. C. Chan, R. W. Sun and T. Zou, *Angew. Chem. Int. Ed.*, 2020, **59**, 11046-11052.
71. M. Mauro, A. Aliprandi, D. Septiadi, N. S. Kehr and L. De Cola, *Chem. Soc. Rev.*, 2014, **43**, 4144-4166.
72. X. Yin, S. A. Warren, Y. T. Pan, K. C. Tsao, D. L. Gray, J. Bertke and H. Yang, *Angew. Chem. Int. Ed.*, 2014, **126**, 14311-14315.
73. K. Li, G. S. Ming Tong, Q. Wan, G. Cheng, W.-Y. Tong, W.-H. Ang, W.-L. Kwong and C.-M. Che, *Chem. Sci.*, 2016, **7**, 1653-1673.
74. T. W. Thomas and A. E. Underhill, *Chem. Soc. Rev.*, 1972, **1**, 99-120.
75. A. Aliprandi, D. Genovese, M. Mauro and L. De Cola, *Chem. Lett.*, 2015, **44**, 1152-1169.
76. Q. Wan, W.-P. To, X. Chang and C.-M. Che, *Chem*, 2020, **6**, 1-23.
77. M.-Y. Yuen, V. A. L. Roy, W. Lu, S. C. F. Kui, G. S. M. Tong, M.-H. So, S. S.-Y. Chui, M. Muccini, J. Q. Ning, S. J. Xu and C.-M. Che, *Angew. Chem. Int. Ed.*, 2008, **47**, 9895-9899.
78. C.-N. Lok, T. Zou, J.-J. Zhang, I. W.-S. Lin and C.-M. Che, *Adv. Mater.*, 2014, **26**, 5550-5557.
79. J. Zhao and M. H. Stenzel, *Polym. Chem.*, 2018, **9**, 259-272.

80. S. Sinn, L. Yang, F. Biedermann, D. Wang, C. Kübel, J. J. L. M. Cornelissen and L. De Cola, *J. Am. Chem. Soc.*, 2018, **140**, 2355-2362.
81. P.-K. Chow, W.-P. To, K.-H. Low and C.-M. Che, *Chem. Asian J.*, 2014, **9**, 534-545.
82. Q. Wan, W.-P. To, C. Yang and C.-M. Che, *Angew. Chem. Int. Ed.*, 2018, **57**, 3089-3093.
83. S. W. Lai, T. C. Cheung, M. C. Chan, K. K. Cheung, S. M. Peng and C. M. Che, *Inorg. Chem.*, 2000, **39**, 255-262.
84. C. Zou, J. Lin, S. Suo, M. Xie, X. Chang and W. Lu, *Chem. Commun.*, 2018, **54**, 5319-5322.
85. Q. Wan, J. Xia, W. Lu, J. Yang and C.-M. Che, *J. Am. Chem. Soc.*, 2019, **141**, 11572-11582.
86. R. A. Freitas, *Nanomedicine*, 2005, **1**, 2-9.
87. B. Y. Kim, J. T. Rutka and W. C. Chan, *N. Engl. J. Med.*, 2010, **363**, 2434-2443.
88. K. Greish, *Enhanced permeability and retention (EPR) effect for anticancer nanomedicine drug targeting*, Cancer nanotechnology, Humana Press, 2010.
89. Y. Shi, R. van der Meel, X. Chen and T. Lammers, *Theranostics*, 2020, **10**, 7921-7924.
90. J. A. Nagy, S. H. Chang, A. M. Dvorak and H. F. Dvorak, *Br. J. Cancer*, 2009, **100**, 865-869.
91. M. Chidambaram, R. Manavalan and K. Kathiresan, *J. Pharm. Pharmaceut. Sci.*, 2011, **14**, 67-77.
92. U. Prabhakar, H. Maeda, R. K. Jain, E. M. Sevick-Muraca, W. Zamboni, O. C. Farokhzad, S. T. Barry, A. Gabizon, P. Grodzinski and D. C. Blakey, *Cancer Res.*, 2013, **73**, 2412-2417.
93. S. Sindhwani, A. M. Syed, J. Ngai, B. R. Kingston, L. Maiorino, J. Rothschild, P. MacMillan, Y. Zhang, N. U. Rajesh, T. Hoang, J. L. Y. Wu, S. Wilhelm, A. Zilman, S. Gadde, A. Sulaiman, B. Ouyang, Z. Lin, L. Wang, M. Egeblad and W. C. W. Chan, *Nat. Mater.*, 2020, **19**, 566-575.
94. Y. Y. Chen, A. M. Syed, P. MacMillan, J. V. Rocheleau and W. C. W. Chan, *Adv. Mater.*, 2020, **32**, e1906274.
95. E. C. Cho, Q. Zhang and Y. Xia, *Nat. Nanotechnol.*, 2011, **6**, 385-391.
96. T. L. Doane and C. Burda, *Chem. Soc. Rev.*, 2012, **41**.
97. C.-W. Lai, Y.-H. Wang, C.-H. Lai, M.-J. Yang, C.-Y. Chen, P.-T. Chou, C.-S. Chan, Y. Chi, Y.-C. Chen and J.-K. Hsiao, *Small*, 2008, **4**, 218-224.
98. L. Zeng, P. Gupta, Y. Chen, E. Wang, L. Ji, H. Chao and Z.-S. Chen, *Chem. Soc. Rev.*, 2017, **46**, 5771-5804.
99. J. Karges, O. Blacque, H. Chao and G. Gasser, *Inorg. Chem.*, 2019, **58**, 12422-12432.
100. J. J. Giner-Casares, M. Henriksen-Lacey, M. Coronado-Puchau and L. M. Liz-Marzán, *Mater. Today*, 2016, **19**, 19-28.
101. E. Boisselier and D. Astruc, *Chem. Soc. Rev.*, 2009, **38**.
102. V. Amendola, R. Pilot, M. Frascioni, O. M. Maragò and M. A. Iatì, *J. Condens. Matter Phys.*, 2017, **29**.
103. L. R. Hirsch, R. J. Stafford, J. A. Bankson, S. R. Sershen, B. Rivera, R. E. Price, J. D. Hazle, N. J. Halas and J. L. West, *Proc. Natl. Acad. Sci. U.S.A.*, 2003, **100**, 13549-13554.
104. A. Narmani, B. Farhood, H. Haghi-Aminjan, T. Mortezaazadeh, A. Aliasgharzadeh, M. Mohseni, M. Najafi and H. Abbasi, *J. Drug Deliv. Sci. Technol.*, 2018, **44**, 457-466.
105. H. Dong, S. R. Du, X. Y. Zheng, G. M. Lyu, L. D. Sun, L. D. Li, P. Z. Zhang, C. Zhang and C. H. Yan, *Chem. Rev.*, 2015, **115**, 10725-10815.
106. B. Chen and F. Wang, *Acc. Chem. Res.*, 2020, **53**, 358-367.
107. Y. Liu, X. Meng and W. Bu, *Coord. Chem. Rev.*, 2019, **379**, 82-98.
108. Y. Liu, D. Tu, H. Zhu and X. Chen, *Chem. Soc. Rev.*, 2013, **42**, 6924-6958.
109. M. S. Meijer, M. M. Natile and S. Bonnet, *Inorg. Chem.*, 2020, **59**, 14807-14818.